Starvation Induced Autophagy Promotes The Progression of Bladder Cancer By LDHA Mediated Metabolic Reprogramming

Tinghao Li
The First Affiliated Hospital of Chongqing Medical University https://orcid.org/0000-0002-7980-6298
Hang Tong
The First Affiliated Hospital of Chongqing Medical University
Hubin Yin
The First Affiliated Hospital of Chongqing Medical University
Yi Luo
The First Affiliated Hospital of Chongqing Medical University
Junlong Zhu
The First Affiliated Hospital of Chongqing Medical University
Zijia Qin
The First Affiliated Hospital of Chongqing Medical University
Siwen Yin
The First Affiliated Hospital of Chongqing Medical University
Weiyang He (202485@hospital.cqmu.edu.cn)
The First Affiliated Hospital of Chongqing Medical University

Research Article

Keywords: Bladder Cancer, Autophagy, Glycolysis, LDHA, Wnt/β-catenin signalling, Axin1

Posted Date: August 23rd, 2021

DOI: https://doi.org/10.21203/rs.3.rs-795270/v1

Abstract

Background: Aberrantly autophagy and preternatural elevated glycolysis are prevalent in bladder cancer (BLCA), which are both related to malignant progression. But the regulatory relationship between autophagy and glycolytic metabolism remains unveiled. We imitated a starvation condition of tumor microenvironment and found significantly increased level of autophagy and aerobic glycolysis, which both regulated progression of BLCA cells. We further explored regulatory relationships and mechanisms between them.

Methods: We used immunoblotting, immunofluorescence and transmission electron microscopy to detect autophagy levels of BLCA cells under different treatment. Lactate and glucose concentration detection demonstrated changes on glycolysis. Expression of lactate dehydrogenase A (LDHA) were detected at transcriptional and translational levels, which were also silenced by small interfering RNA and effects on malignant progression further tested. Underlying mechanisms on signaling pathways were performed by western blot, immunofluorescence and immunoprecipitation assays.

Results: Starvation induced autophagy, regulated glycolysis by up-regulating expression of LDHA and caused progressive changes in BLCA cells. Mechanically, after starved ubiquitination modification of Axin1 increased and combined with P62, further degraded by autophagy-lysosome pathway. Liberated β-catenin nuclear translocation increased, binding with LEF1/TCF4 and promotes LDHA transcriptional expression. Also, high expression of LDHA was observed in cancer tissues and positively related to progression.

Conclusion: Our study demonstrated that starvation-induced autophagy modulates glucose metabolic reprogramming by enhances Axin1 degradation and β-catenin nuclear translocation in BLCA, which promotes transcriptional expression of LDHA and further malignant progression.

Background

Bladder cancer (BC) is the second most common genitourinary tumour, with over 430,000 patients diagnosed worldwide yearly[1]. Cancer cells always live in a tumour microenvironment (TME) with intermittent starvation, hypoxia, and inflammatory microenvironments due to excessive multiplication and lack of vascular perfusion[2]. Cancer cells' unlimited proliferation and hyper-adaptation to drastic changes are generally maintained by adaptive metabolic reprogramming caused by harsh living conditions, accelerating the development of cancer cells[3-5]. The conflict between the deprivation of nutrients and the promotion of their malignancies has attracted great attentions. Thus, the effects of TME on BC cells remain to be addressed.

Autophagy acts as a cancer suppressor in normal tissues while it is over-activated to counteract different kinds of adverse conditions in cancer cells[6]. Autophagy plays a protective role in BC cells under the conditions of intermittent starvation or hypoxia. The autophagic process can be explained in two steps: Firstly, autophagosomes degrade the ribosomal region of the rough endoplasmic reticulum, breaking

down cargos like redundant proteins and organelles. Then, autophagosomes fuse with lysosomes to form autophagy lysosomes for further degradation. This facilitates the cycling and reutilization of materials and energies[7-9]. The effects of hostile TME on autophagy and the influence of elevated autophagy on cancer cells remain unknown. Epigenetic modification on metabolic reprogramming is one such way. It is known that cells require three main nutrients for survival, and under nutrient deprivation, cancer cells could reprogram their metabolic ways. This is sometimes triggered by enhanced autophagy and leads to malignant progression[10, 11].

Glycolysis is a characteristic feature of tumour cells, which is termed as Warburg effect. The mechanisms of glycolysis and key enzymes and regulators of glycolytic pathways have drawn wide attention recently. It was reported that regulation of key enzymes in glycolysis at transcriptional or translational levels affects both the transformations on glucose metabolism and the progressive transformations of cancer cells. Starvation could promote the translational expression of MCT1 by upregulated autophagy and accelerate metastasis in hepatic cancer[12]. PFKP was also known to have a core role in the malignant process in oral squamous cell carcinoma[13]. This study aimed at investigating the connections between aberrant autophagy and enhanced aerobic glycolysis in BC.

The findings of this study revealed that transient starvation could enhance autophagic flux. This is achieved by accelerating the ubiquitin-mediated degradation of Axin1 and liberating the transcriptional expression of key enzyme LDHA (lactate dehydrogenase A) to modulate the levels of glycolysis, allowing the malignant progression of BC.

Materials And Methods

Cell culture and treatment

Two strains of BC cells (T24 and UM-UC-3) were obtained from American Type Culture Collection (Manassas, VA). Normal treated groups were grown in complete medium supplemented with 10% fetal bovine serum (Gibco, Thermo Fisher Scientific, MA). Starvation incubated groups were treated by Hank's balanced salt solution (HBSS; Boster Biotechnology, Wuhan, China) for six hours and then recovered in complete medium for further experiments. Chloroquine (CQ, 20 mM; Sigma-aldrich, USA), 3-methyladenine (3-MA, 5 mM; Selleck Chemicals, Houston, TX), 2-Deoxy-D-glucose (2-DG, 5 mM; Selleck Chemicals), MG132 (50 mM; Selleck Chemicals) and PNU-74654 (50 mM; Selleck Chemicals) were used to treat cell lines for different inhibitions.

Small interfering RNA interference assay

All small interfering RNAs (siRNAs) targeting human LDHA or negative control were designed and synthetized by GenePharma (Shanghai, China), transfected into the cell lines with Lipofectamine 2000 (Invitrogen, Carlsbad, CA), according to the manufacturer's instructions. Sequences were demonstrated in Table1.

Quantitative real-time polymerase chain reaction

Total RNA was drawn out from T24 or UM-UC-3 cells processed by different experimental conditions. PrimeScript RT reagent kit (TaKaRa, Osaka, Japan) were used to reverse-transcribe RNA (1 mg) to cDNA. Real-time qPCR was performed with SYBR Green (TaKaRa) on an ABI 7500 Real-Time PCR System (Applied Biosystems), the entire process followed the manufacturer's instructions. Data were standardized to β-actin using the $2^{-\Delta\Delta Ct}$ method. The primer sequences were demonstrated in Table 1.

Immunoblots

Total protein was drawn out using radioimmunoprecipitation assay lysis buffer (Beyotime, China). NE-PER^{TM} Nuclear Cytoplasmic Extraction Reagent kit (Thermo Fisher Scientific, MA) were used according to the manufacturer's instruction for extracting protein of nuclear and cytoplasmic from different groups.

12% sodium dodecyl sulfate-polyacrylamide gel was chosen for total protein separation and transferred to nitrocellulose membranes (Millipore, USA). Membranes were incubated with primary antibodies including: anti-LC3B (Abcam Cat# ab192890, RRID:AB_2827794), anti-P62/SQSTM1 (Abcam Cat# ab207305, RRID:AB_2885112), anti-β-actin (Proteintech# 20536-1-AP), anti-LDHA (Cell Signaling Technology Cat# 3582,RRID:AB_2066887), anti-β-catenin (Cell Signaling Technology Cat# 8480), anti-p-β-catenin (Cell Signaling Technology Cat# 4176), anti-c-Myc (Covance Cat# MMS-150P-1000,RRID:AB_291322), anti-GSK3-β (Cell Signaling Technology Cat# 121456), anti-Axin1 (Cell Signaling Technology Cat# 2087,RRID:AB_2274550) and anti-Histone H3 (Cell Signaling Technology Cat# 4499,RRID:AB_10544537). Enhanced chemiluminescence reagents (Millipore, USA) were used to assess protein expression.

Cell proliferation and viability

Cell proliferation was demonstrated by Cell Counting Kit-8 (CCK8, Boster Biotechnology) and colony formation assay. For CCK8 assay, cells were inoculated onto 96-well plates. CCK8 reagent was added 10 ml to each well at different timings. For colony formation assay, cells were inoculated onto 6- and 24-well plates with complete medium for 10 days, at a density of 500 cells per well when inoculating to 6-well plate, and 100 cells per well for 24-well plate. Colonies were fixed with 4% paraformaldehyde fix solution (P0099, Beyotime, China) and stained by 0.1% crystal violet staining solution (C0121, Beyotime).

Cell activity, used to reflect the sensitivity of cells to chemotherapy, was also presented by CCK8 assay. In accordance with the methods and procedures mentioned above, different groups were inoculated onto 96-well plates and treated with cisplatin at the indicated concentrations (0, 0.2, 0.5, 1, 2, 5, 10 and 20 μM) for further 48h incubation.

Transwell migration and invasion assays

The migration and invasion assay were performed using a 24-well Transwell chamber. For the migration assay cells were inoculated in the upper chamber. Migrated cells that attached to the substratum of the

membrane were observed and photographed after fixation and staining. To evaluate the migration abilities of different groups, migrated cells on each chamber were counted 5 isolated fields under a 200-fold microscope. For the invasion assay, 50 ml matrigel mixture was added to the upper chamber in advance. The rest procedures and methods are the same as above.

Lactate production and glucose consumption measurement

Lactate and glucose concentrations in the culture supernatants were detected using Lactate Assay kit (Solarbio, Beijing, China) and Glucose Assay kit (Solarbio) respectively, according to the manufacturer's instructions and absorbance values were measured at the corresponding absorbance. The results were normalized by the number of cells in each sample in the culture plates, lactate production and glucose consumption were calculated by comparison with normal medium.

Transmission electron microscopy

Cells were fixed in 3% glutaraldehyde electron microscope fixation solution, after gradually dehydrated by 50-100% ethanol gradient and embedded by araldite. Samples were chopped into ultrathin sections and stained with uranyl acetate and lead citrate. Images were obtained by transmission electron microscope.

Immunofluorescence

Cells were fixed for 30 mins. After permeabilized with 1% Triton X-100, primary including anti-LC3B (Abcam Cat# ab192890, RRID: AB_2827794) or anti-β-catenin (Cell Signaling Technology Cat# 8480) was added. Secondary antibody Alexa 488-conjugated goat anti-rabbit IgG (Beyotime Cat# A0423, RRID: AB_2891323) was added. After counterstained with DAPI (Beyotime Cat# C1002), cells were observed under a confocal microscope.

Immunoprecipitation (IP) and ubiquitination assay

Cells were harvested and lysed by IP lysis buffer (Beyotime Cat# P0013). Samples were centrifuged, supernatants were collected and 2.5mg of anti-Axin1 (Cell Signaling Technology Cat# 2087, RRID: AB_2274550), anti-p62 (Abcam Cat# ab207305, RRID: AB_2885112) or anti-IgG (Cell Signaling Technology Cat# 3900S) antibodies were added. Protein A/G immunoprecipitation beads were added to the suspension. Beads binding proteins were isolated by magnetic grate. IgG was used as negative control. For detecting and inhibiting ubiquitin protein, anti-Ubiquitin (Cell Signaling Technology Cat# 3933, RRID: AB_2180538) and MG132 (Selleck Chemicals Cat# S2619) 20mM dissolved with DMSO were also selected and applied.

Animal experiments

BALB/c nude mice (HFKBIO, Beijing, China) were fed under standard conditions. 5×10^6 cells with normal or starvation treatment were subcutaneously inoculated. Measurements were taken every 3 days on the tumor volume which was calculated as: tumor volume (mm^3) =0.5×longest diameter× shortest $diameter^2$.

Till the average tumor volume reached 30mm^3, equal amount of CQ (50mg/ml dissolved in 0.9% saline, Sigma-aldrich) or 0.9% saline was then administered intraperitoneally every 3 days. Two weeks later, the mice were suffocated to euthanasia by high concentration of carbon dioxide after 3% pentobarbital sodium deep anesthesia, the size of the tumors were recorded for further analysis.

Clinical data for human tissue specimens and bioinformatic analysis

Fifteen pairs cancer tissues and adjacent tissues of patients who underwent radical cystectomy for BC were collected in The First Affiliated Hospital of Chongqing Medical University. For bioinformatic analysis, immunohistochemical (IHC) images about the expression of LDHA in normal urothelial and urothelial cancer cells were downloaded from Human Protein Atlas database.

Statistical analysis

Experiments were independently repeated and representative images are performed in figures. Results of analyses are performed as the mean ± standard deviation. Unpaired students *t* tests were performed to compare the differences between two groups. Data of multiple groups results were analysed by Mann-Whitney test. P value<0.05 was considered statistically significant and significance levels were set to p^{*} <0.05, p^{**}<0.01, p^{***}<0.001 or nonsignificant (ns).

Results

Microenvironment of Starvation Enhances the Malignant Progression of BC

BC cells were treated with Hank's buffered salt solution (HBSS) for six hours[14]. After starvation, the ability of proliferation was promoted compared to the controlled group in the CCK-8 assay (Figure 1A). This finding was also confirmed by the clone formation assay (Figure 1B). As shown in Figure 1C, the ability to migrate was enhanced after starvation. The invasion was also promoted significantly relative to the normal cultured group. Cisplatin was selected as the drug delivery reagent in the drug sensitivity test since its widely applied in chemotherapy of BC patients. With the use of CCK-8 assay, T24 and UM-UC-3 cells were found to be exhibiting higher resistance to cisplatin after starvation (Figure 1D).

Starvation-induced autophagy promotes the progression of BC

Both transmission electron microscope and confocal microscopy were used to observe the formation of autophagosomes in T24 cells. In the starvation group, more autophagosomes and more aggregations of LC3B in the cytoplasm were observed (Figure 2A, B). The expression of P62 and LC3-II were detected, which confirmed that autophagic flux was blocked by Chloroquine (CQ) in the late stages or 3-Methyladenine (3-MA) in early-stage (Figure 2C, Sfigure A). CCK-8 assay demonstrated that after being incubated with HBSS and CQ, the proliferation of T24 cells was significantly inhibited at 48h and 72h in contrast to the starvation-only group (Figure 2D). Subsequently normal or starvation incubated T24 cells were subcutaneously inoculated into nude mice at the same time. The routine culture was carried out and

equal amounts of CQ or 0.9% saline was administered intraperitoneally. It was observed that all starvation group cells grew faster than normal group cells before intraperitoneal injection.After injected with CQ, the tumours' growth rate of the starved group was significantly inhibited (Figure 2E, F). BC cells' invasion and migration abilities were significantly increased after starvation compared to the control group cells and the cells treated with CQ. However, CQ incubated only group didn't represent variation (Figure 2G, H).

Starvation-induced autophagy regulates BC glucose metabolic reprogramming by transcriptional overexpression of LDHA

Glucose consumption and lactate production rates were measured. As shown in Figure 3A, T24 and UM-UC-3 cells both exhibited significantly higher glycolysis levels after starvation ($P<0.05$). Then, inhibitors were added to block autophagic flux. The results demonstrated that after disposed by CQ or 3-MA, the glycolysis level of T24 cells was significantly inhibited (Figure 3B, Sfigure B). Exclusive glycolytic inhibitor 2-Deoxy-D-glucose (2-DG) was selected to verify the significant increase in glycolytic levels. The glycolysis level of BC cells was significantly inhibited after HBSS coprocessing with 2-DG (Figure 3C).

Then, western-blot and immunofluorescent staining were used to investigate the effects of inhibiting glycolysis on autophagy. No significant changes were detected on either degradation of P62 or decompose of LC3B after starvation plus 2-DG (Figure 3D), the same as aggregation of LC3B in the cytoplasm (Figure 3E).

The expression of several key enzymes of glycolysis were probed at the transcriptional level in normal and HBSS treated groups, including G6PD (glucose-6-phosphate dehydrogenase), GLUT1 (glucose transporter type 1), HK2 (hexokinase 2), LDHA, PDK1 (Pyruvate dehydrogenase kinase isoenzyme 1), PFKP (phosphofructokinase, platelet). *LDHA* was found to be upregulated most obviously (Figure 3F). The overexpression of LDHA at transcriptional and translational levels induced by starvation was verified by RT-qPCR and western-blot. After co-treated by CQ, the expression of LDHA was inhibited significantly with or without starvation (Figure 3G).

Starvation-induced metabolic reprogramming promotes the progression of BC by LDHA.

With the use of either CQ or 2-DG, BC cells' starvation-induced proliferation was inhibited in the CCK-8 and clone formation assay (Figure 4A). When measuring the migration ability, the same trend was observed in the transwell and wound healing assay (Figure 4B). These results indicate that starvation-induced autophagy may regulate glucose metabolic reprogramming by affecting the expression of LDHA on transcription levels. Small interfering RNAs (siRNAs) targeting LDHA were constructed to evaluate their role in the progression of BC cells under starvation. RT-qPCR and western-blot were both used to examine the efficiency of three siRNA sequences (Figure 4C, Sfigure C).

T24 cells were selected to inhibit the expression of LDHA. Changes of glycolysis levels and their effects on progression in different groups were evaluated. Firstly, silencing LDHA suppressed starvation-induced

glycolysis. The second sequence, in particular, exhibited the strongest inhibition on glucose consumption and lactate production (Figure 4D). Secondly, the impacts of silencing LDHA on the starvation-induced progression of BC cells were examined. Results suggested that starvation induced BC cells progression were suppressed via silencing LDHA (Figure 4E-H).

Overexpression of LDHA is closely related to clinical BC patients

Metabolism reprogramming is one of the main hallmarks of cancer cells[15]. The common mutation sites and structures were predicted by cBioportal (Sfigure D). As shown in Figure 5A, mutations in LDHA were widespread in different cancers including BC. One such mutation in BC is amplification. Immunohistochemical images of normal and cancer urothelium tissue were downloaded from the Human Protein Atlas database. Squamous epithelial cells of tumour tissues showed significantly higher LDHA staining than normal (Figure 5B). RNA was extracted from 15 BC patients' cancer and adjacent tissues. Results showed that *LDHA* was overexpressed in cancer tissues at transcriptional levels (Figure 5C). Next, eight specimens were randomly sampled from 15 patients to extract protein and detected the expression of LDHA protein (Figure 5D).

In Cohort Dyrskjot Bladder 3, comprised of 60 BC patients with different depths of infiltration, demonstrated that higher LDHA was expressed with deeper infiltration tissues (Figure 5E). Transcriptome data of 378 BC patients downloaded from the Cancer Genome Atlas (TCGA) database were analyzed, and LDHA mRNA expression correlated positively with ATG5 mRNA ($r=0.61$, $p<0.001$) (Figure 5F).

Starvation Regulates Expression of LDHA Through Canonical Wnt/β-catenin Pathway

Gene set enrichment analysis (GSEA) demonstrated that the expression or function of LDHA was associated with the Wnt signalling pathway (Figure 6A). With the use of the University of California Santa Cruz Genome Browser and JASPAR, the transcription factor binding site and transcription factors of LDHA were predicted. LEF1 (lymphoid enhancer factor 1) and TCF4 (T-cell factor 4) aroused our attention (Figure 6B) for their high probabilities of binding to the LDHA transcription factor binding site (TFBS). These factors are members of TCF/LEF family that β-catenin specifically binds to and activates the transcription of canonical Wnt pathway target genes[15]. β-catenin functions through binding with TCF/LEF families and enhancing expression of the Wnt target genes[17]. To verify this prediction, firstly, PNU-74654 was chosen to selectively block the combination of β-catenin and TCF/LEF[18]. No differences in the mRNA expression of *CTNNB1* were detected among the three groups. However, *LDHA* mRNA expression was enhanced significantly by starvation and inhibited by PNU-74654 (Figure 6C). Figure 6D demonstrates the overexpression of LDHA by starvation. PNU-74654 didn't impair autophagy flux which was reflected by P62. Combined with RT-qPCR results we believed that the degradation of β-catenin also reverted when T24 cells were treated by HBSS with PNU-74654. Then, proteins were isolated and transformed into cytoplasm and nucleus. Glyceraldehyde 3-phosphate dehydrogenase (GAPDH) and Histon H3 were chosen as loading controls. Western-blot assay demonstrated that β-catenin remained higher after starvation (Figure 6E). Starvation group showed significant intranuclear high aggregation of β-catenin with the use of immunofluorescence, while expression of β-catenin in the control group was

diffused and mainly located in the cytoplasm. After inhibited autophagy by CQ, the process of starvation-induced β-catenin nuclear transposition was blocked (Figure 6F). Nuclear transfer of β-catenin mainly depends on the reduction of phosphorylation modification. Consequently, the phosphorylation levels of β-catenin and c-Myc were observed. After starvation, the total protein expression of β-catenin, c-Myc, and LDHA were all increased; the phosphorylation of β-catenin was decreased (Figure 3G and 6G). Besides the CTNNB1 expression, there were no differences among these groups (Sfigure E).

Starvation Regulates Wnt/β-catenin Pathway by Ubiquitination of Axin1 and Promotion of Autophagy

In the canonical model of Wnt signalling glycogen synthase kinase 3 (GSK3)-dependent phosphorylation marks the β-catenin for degradation at key amino-terminal Ser and Thr residues[19]. Axin1 is considered to be a concentration-limiting factor for the assembly of the β-catenin destruction complex. Degradation of Axin1 enhances the Wnt/β-catenin signalling pathway and increases the expression of downstream genes[20]. We evaluated Axin1 and GSK3-β with the use of autophagy-lysosomal early and final stage inhibitor 3-MA and CQ in the presence and absence of starvation. The results revealed that after starvation the expression of LDHA and stabilization of β-catenin were enhanced, which were reversed after autophagic inhibition. Moreover, with blocking autophagic flux at different stages, the degradation of Axin1 could be all suspended; nevertheless, no indication was found regarding GSK3-β's potential involvement with the Wnt/β-catenin signalling activating process during starvation (Figure 7A).

Ubiquitylation level of proteins in both total and Axin1 was detected (Figure 7B, C). Findings indicated that the ubiquitin modification of Axin1 was increased. Furthermore, the degradation of Axin1 brought into correspondence with P62 (Figure 7B). P62 played a crucial role in targeting autophagy cargos and autophagosomes for degradation, especially proteins with ubiquitin modification(18). After inhibited by CQ, the ubiquitin modification on the total protein was demonstrated to be upregulated relative to the control group; no change was observed compared to the starvation-only group (Figure 7D). In contrast, with increased degradation of Axin1 and P62 after starvation, inhibition of the autophagy lysosomal pathway by CQ also inhibited the degradation of these proteins. Although MG132 did block the ubiquitin-proteasome system pathway, the degradation of Axin1 and P62 protein were not obstructed (Figure 7D). Taken together, these results indicated that starvation-induced autophagy regulated the degradation of ubiquitin-modified Axin1 and released the suppression of the canonical Wnt/β-catenin signalling by decreasing β-catenin phosphorylation. These results confirm a potential relationship between P62 and Axin1. Forecasted by GeneMANIA, protein-protein network results showed no correlation between these two proteins (Sfigure F), which was further confirmed by forward and reverse immunoprecipitation in normal T24 cells (Figure 7E). However, an interaction between P62 and Axin1 in T24 cells was detected after being processed by HBSS. These findings confirm a model of glucose metabolic reprogramming of BC cells induced by starvation-induced autophagy (Figure. 7F).

Discussion

Previous studies in our group had focused on starvation-induced EMT (epithelial-mesenchymal transition) of BC[14]. This study explored the process of metabolic reprogramming induced by autophagy and analyzed the interaction between ubiquitinated Axin1, the skeleton protein of the APC complex, and P62/SQSTM1, a receptor for autophagy cargos[21], for further degradation by the autophagy-lysosome pathway. Autophagy is a double-edged sword for cancer cells. It can result in their survival or death under different circumstances[22]. Hypoxia-induced autophagy could potentially enhance the drug resistance of BC to cisplatin[7], and starvation-induced autophagy promotes its metastasis[14]. Several theories have been proposed to explain the progression of cancer induced by aberrant autophagy. Regarding the progression of cancer as a stress-response mechanism is a reasonable explanation[23]. Insufficient angiogenesis usually makes solid tumour cells outgrow the blood supply. This shortage of nutrients and oxygen resulted from TME generally leads to autophagy. It is important to note that autophagy could promote cancer cells' survival under starvation conditions by recycling intracellular components to support metabolism in the absence of extracellular nutrients[24]. Autophagy often regulates the metabolism of cancer cells in three ways: providing the obligate substrates for energy needs, regulating mitochondrial metabolism to modulate the supply of energy, and activating key enzyme expression in metabolic pathways[25]. Therefore, it would be reasonable to speculate that autophagy alters metabolic reprogramming by regulating key metabolic enzymes. For instance, autophagy downregulates PtdCho and PtdE biosynthesis in the lipid metabolism of gliomas[26]. Other examples are the decreased expression of arginosuccinate synthase 1 enzyme caused by systemic deletion of ATG7 in arginine circulating[26] and the regulated key enzymes expression on glucose metabolism.

The Metabolic patterns of cancer cells are abnormal. They partly acquire energy and components by aerobic glycolysis, and accumulating evidence suggests that glucose metabolic reprogramming is closely related to the malignant progression of cancer cells[2]. Several previous studies have suggested key enzymes like PFKP or GLUT1 could promote or inhibit autophagic flux[13, 27], even though most theories argue that autophagy plays a regulatory role in the expression and activity of key enzymes in glycolysis[28, 29]. In this study, after starvation was processed, BC cells improved their aerobic glycolysis, which could be reversed by inhibition of autophagy. However, when a specific glycolysis inhibitor 2-DG co-treated with starvation was selected, no effects were observed on autophagy. To analyze specific mechanisms, glycolysis-related enzymes in BC cells were detected. The results suggested abnormally overexpression of LDHA.

LDHA is a rate-limiting enzyme of glycolysis that catalyzes the production of lactate, which is relevant to the malignant biological behaviours in diverse cancers[30, 31]. LDHA was silenced by siRNA, and results demonstrated a potential obstacle to BC progression. With the use of bioinformatics tools and clinical samples, it was found that the overexpression of LDHA is correlated with not only carcinogenesis but also malignant progression and enhanced autophagy in BC. The promoter region of LDHA contains multiple elements that could bind with diverse transcription factors[32]. β-catenin is an important second messenger of the canonical Wnt signalling and activates the transcription of Wnt target genes[33]. In the absence of Wnt ligands, β-catenin would be confined to the cytoplasm and rapidly sequestered by a destruction complex consisting of Axin1, GSK3, APC, and CK1, subsequently marked by GSK3-dependent

phosphorylation for further degradation[34]. Axin1 scaffold determines the efficacy of the destruction complex[35]. After observed the aggregation in the nucleus of β-catenin, reduction of phosphorylated β-catenin, and activation of canonical Wnt/β-catenin signalling pathway, it was confirmed that starvation-induced autophagy activated LDHA overexpression by destroying the APC complex. Then, two dominant proteins forming the APC complex were detected after blocking autophagic flux at different stages. Protein SQSTM1/P62 plays numerous roles in autophagic flux as a receptor for autophagy cargo. It was also found to be mediating the degradation of Axin1 via the autophagy-lysosome pathway.

Conclusion

Our study demonstrated that during starvation, ubiquitination modification of Axin1 increased and combined with P62 for further autophagy-lysosome degradation. Depolymerized destruction complex liberated β-catenin and promoted its nuclear translocation, binding with LEF1/TCF4 and causing glucose metabolic reprogramming and further progressive changes in BC cells. Future research should certainly further investigate why ubiquitination modification on Axin1 increases under starvation conditions and how LDHA induces BC's progressive transformation.

Declarations

Ethics Statement

The study was approved by the Ethics Committee of the First Affiliated Hospital of Chongqing Medical University (Chongqing, China).

Consent for publication

Not applicable

Availability of data and materials

Not applicable

Acknowledgements

The authors gratefully acknowledge the assistance of the Department of Urology Surgery.

Competing interests

There are no financial disclosures or competing interests among authors.

Funding

This study was supported by funds from the Natural Science Foundation of China (Grant No. 81874092).

Author Contribution Statement

HWY and LTH conceived and designed the study. LTH and TH performed all the experiments. QZJ and YSW collected the data. ZJL interpreted and analyzed the data. LY, TH, and YHB wrote the manuscript. YHB and LTH revised the manuscript critically.

References

1. Patel VG, Oh WK, Galsky MD. Treatment of muscle-invasive and advanced bladder cancer in 2020. CA Cancer J Clin. 2020;70(5):404–23.
2. Yoshida GJ. Metabolic reprogramming: the emerging concept and associated therapeutic strategies. J Exp Clin Cancer Res. 2015;34:111.
3. Kurtova AV, Xiao J, Mo Q, Pazhanisamy S, Krasnow R, Lerner SP, Chen F, Roh TT, Lay E, Ho PL, et al. Blocking PGE2-induced tumour repopulation abrogates bladder cancer chemoresistance. NATURE. 2015;517(7533):209–13.
4. Koay EJ, Truty MJ, Cristini V, Thomas RM, Chen R, Chatterjee D, Kang Y, Bhosale PR, Tamm EP, Crane CH, et al. Transport properties of pancreatic cancer describe gemcitabine delivery and response. J CLIN INVEST. 2014;124(4):1525–36.
5. Damaghi M, West J, Robertson-Tessi M, Xu L, Ferrall-Fairbanks MC, Stewart PA, Persi E, Fridley BL, Altrock PM, Gatenby RA, et al: **The harsh microenvironment in early breast cancer selects for a Warburg phenotype**. *Proc Natl Acad Sci U S A* 2021, 118(3).
6. Rybstein MD, Bravo-San PJ, Kroemer G, Galluzzi L. The autophagic network and cancer. NAT CELL BIOL. 2018;20(3):243–51.
7. Mao X, Nanzhang, Xiao J, Wu H, Ding K. Hypoxia-Induced Autophagy Enhances Cisplatin Resistance in Human Bladder Cancer Cells by Targeting Hypoxia-Inducible Factor-1α. J IMMUNOL RES. 2021;2021:8887437.
8. Ojha R, Singh SK, Bhattacharyya S, Dhanda RS, Rakha A, Mandal AK, Jha V. Inhibition of grade dependent autophagy in urothelial carcinoma increases cell death under nutritional limiting condition and potentiates the cytotoxicity of chemotherapeutic agent. J Urol. 2014;191(6):1889–98.
9. Mizushima N, Levine B. Autophagy in Human Diseases. N Engl J Med. 2020;383(16):1564–76.
10. VandeKopple MJ, Wu J, Auer EN, Giaccia AJ, Denko NC, Papandreou I. HILPDA Regulates Lipid Metabolism, Lipid Droplet Abundance, and Response to Microenvironmental Stress in Solid Tumors. MOL CANCER RES. 2019;17(10):2089–101.
11. Nowosad A, Jeannot P, Callot C, Creff J, Perchey RT, Joffre C, Codogno P, Manenti S, Besson A. p27 controls Ragulator and mTOR activity in amino acid-deprived cells to regulate the autophagy-lysosomal pathway and coordinate cell cycle and cell growth. NAT CELL BIOL. 2020;22(9):1076–90.
12. Fan Q, Yang L, Zhang X, Ma Y, Li Y, Dong L, Zong Z, Hua X, Su D, Li H, et al. Autophagy promotes metastasis and glycolysis by upregulating MCT1 expression and Wnt/β-catenin signaling pathway activation in hepatocellular carcinoma cells. J Exp Clin Cancer Res. 2018;37(1):9.

13. Chen G, Liu H, Zhang Y, Liang J, Zhu Y, Zhang M, Yu D, Wang C, Hou J. Silencing PFKP inhibits starvation-induced autophagy, glycolysis, and epithelial mesenchymal transition in oral squamous cell carcinoma. EXP CELL RES. 2018;370(1):46–57.
14. Tong H, Yin H, Hossain MA, Wang Y, Wu F, Dong X, Gao S, Zhan K, He W. Starvation-induced autophagy promotes the invasion and migration of human bladder cancer cells via TGF-β1/Smad3-mediated epithelial-mesenchymal transition activation. J CELL BIOCHEM. 2019;120(4):5118–27.
15. Pavlova NN, Thompson CB. The Emerging Hallmarks of Cancer Metabolism. CELL METAB. 2016;23(1):27–47.
16. van Amerongen R. **Alternative Wnt pathways and receptors**. *Cold Spring Harb Perspect Biol* 2012, 4(10).
17. Doumpas N, Lampart F, Robinson MD, Lentini A, Nestor CE, Cantù C, Basler K. **TCF/LEF dependent and independent transcriptional regulation of Wnt/β-catenin target genes**. *EMBO J* 2019, 38(2).
18. Buikema JW, Lee S, Goodyer WR, Maas RG, Chirikian O, Li G, Miao Y, Paige SL, Lee D, Wu H, et al. Wnt Activation and Reduced Cell-Cell Contact Synergistically Induce Massive Expansion of Functional Human iPSC-Derived Cardiomyocytes. CELL STEM CELL. 2020;27(1):50–63.
19. Ji L, Jiang B, Jiang X, Charlat O, Chen A, Mickanin C, Bauer A, Xu W, Yan X, Cong F. The SIAH E3 ubiquitin ligases promote Wnt/β-catenin signaling through mediating Wnt-induced Axin degradation. Genes Dev. 2017;31(9):904–15.
20. Deng R, Zuo C, Li Y, Xue B, Xun Z, Guo Y, Wang X, Xu Y, Tian R, Chen S, et al. The innate immune effector ISG12a promotes cancer immunity by suppressing the canonical Wnt/β-catenin signaling pathway. CELL MOL IMMUNOL. 2020;17(11):1163–79.
21. Komatsu M. Potential role of p62 in tumor development. AUTOPHAGY. 2011;7(9):1088–90.
22. Shintani T, Klionsky DJ. Autophagy in health and disease: a double-edged sword. SCIENCE. 2004;306(5698):990–5.
23. Deng S, Shanmugam MK, Kumar AP, Yap CT, Sethi G, Bishayee A. Targeting autophagy using natural compounds for cancer prevention and therapy. CANCER-AM CANCER SOC. 2019;125(8):1228–46.
24. Rabinowitz JD, White E. Autophagy and metabolism. SCIENCE. 2010;330(6009):1344–8.
25. Madrigal-Matute J, Cuervo AM. Regulation of Liver Metabolism by Autophagy. GASTROENTEROLOGY. 2016;150(2):328–39.
26. Poillet-Perez L, Xie X, Zhan L, Yang Y, Sharp DW, Hu ZS, Su X, Maganti A, Jiang C, Lu W, et al. Autophagy maintains tumour growth through circulating arginine. NATURE. 2018;563(7732):569–73.
27. Sun M, Zhao S, Duan Y, Ma Y, Wang Y, Ji H, Zhang Q. GLUT1 participates in tamoxifen resistance in breast cancer cells through autophagy regulation. Naunyn Schmiedebergs Arch Pharmacol. 2021;394(1):205–16.
28. Jiao L, Zhang HL, Li DD, Yang KL, Tang J, Li X, Ji J, Yu Y, Wu RY, Ravichandran S, et al: **Regulation of glycolytic metabolism by autophagy in liver cancer involves selective autophagic degradation of HK2 (hexokinase 2)**. *AUTOPHAGY* 2018, **14**(4):671–684.

29. Roy S, Leidal AM, Ye J, Ronen SM, Debnath J. Autophagy-Dependent Shuttling of TBC1D5 Controls Plasma Membrane Translocation of GLUT1 and Glucose Uptake. MOL CELL. 2017;67(1):84–95.
30. Le A, Cooper CR, Gouw AM, Dinavahi R, Maitra A, Deck LM, Royer RE, Vander JD, Semenza GL, Dang CV. Inhibition of lactate dehydrogenase A induces oxidative stress and inhibits tumor progression. Proc Natl Acad Sci U S A. 2010;107(5):2037–42.
31. Liu X, Yao D, Liu C, Cao Y, Yang Q, Sun Z, Liu D. Overexpression of ABCC3 promotes cell proliferation, drug resistance, and aerobic glycolysis and is associated with poor prognosis in urinary bladder cancer patients. Tumour Biol. 2016;37(6):8367–74.
32. Feng Y, Xiong Y, Qiao T, Li X, Jia L, Han Y. Lactate dehydrogenase A: A key player in carcinogenesis and potential target in cancer therapy. Cancer Med. 2018;7(12):6124–36.
33. Niehrs C. The complex world of WNT receptor signalling. Nat Rev Mol Cell Biol. 2012;13(12):767–79.
34. Mosimann C, Hausmann G, Basler K. Beta-catenin hits chromatin: regulation of Wnt target gene activation. Nat Rev Mol Cell Biol. 2009;10(4):276–86.
35. Takebe N, Miele L, Harris PJ, Jeong W, Bando H, Kahn M, Yang SX, Ivy SP. Targeting Notch, Hedgehog, and Wnt pathways in cancer stem cells: clinical update. NAT REV CLIN ONCOL. 2015;12(8):445–64.

Tables

Due to technical limitations, table 1 is only available as a download in the Supplemental Files section.

Figures

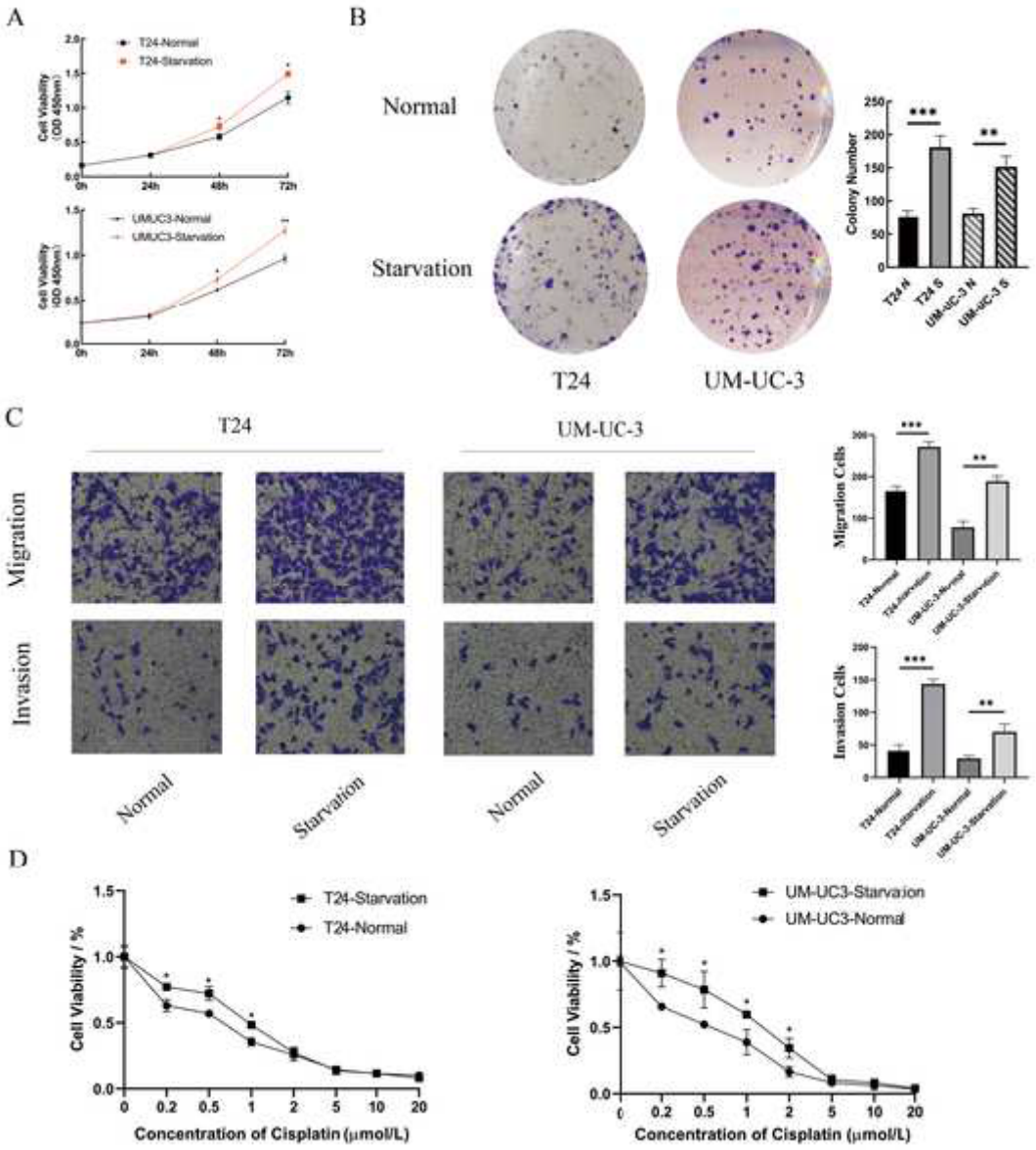

Figure 1

Microenvironment of Starvation Enhanced the Malignant Progression of BC. a. Viability of two strains BC cells after six hours normal or HBSS treatment were measured at 0, 24, 48 and 72h respectively (n=3, Mann-Whitney test, P* < 0.05). b. Colony forming assay were demonstrated the proliferation abilities of T24 and UM-UC-3 cells treated with or without starvation (n=3, unpaired students T test, P** < 0.01, P*** < 0.001). c. Cell transwell migration and invasion assay were chosen to detect the migration and invasion abilities between normal and starvation groups. d. Viabilities of two strains with different treatments were measured after processing with graded concentrations of cisplatin 48h (n=3, non-parametric Mann-Whitney test, P* < 0.05).

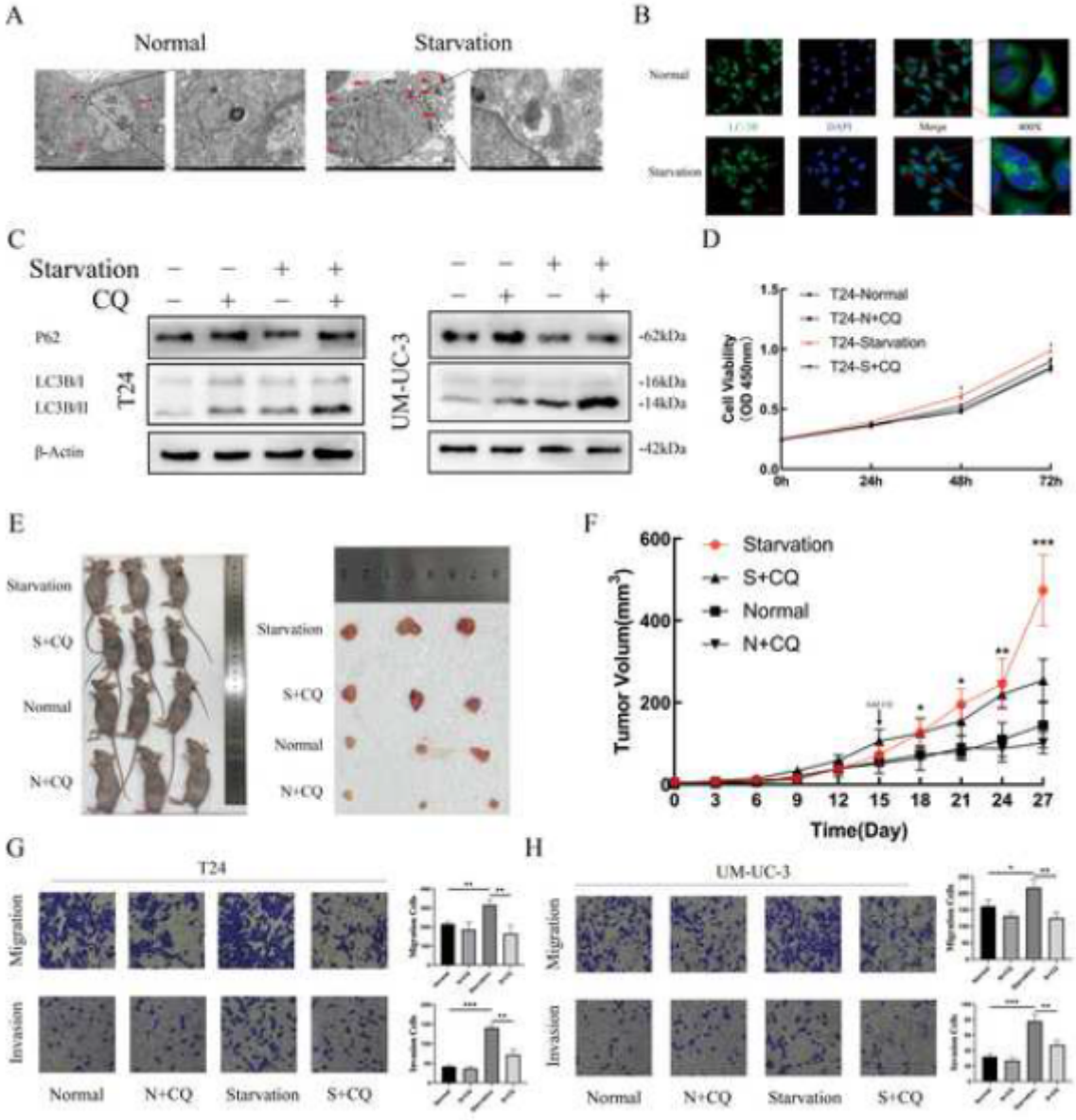

Figure 2

Starvation-induced Autophagy Promoted the Progression of BC. a. After normal or HBSS treatment, T24 cells were fixed and the formation of autophagosomes were observed by transmission electron microscopy. Autophagosomes marked by Red Arrows (scale bar, 2mm). b. Immunofluorescence staining of LC3B was performed in T24 cells with normal or HBSS treatment, the aggregation of LC3B represented the formation of autophagosomes. c. Western-blot were used to detect the expression of LC3B-I/II and SQSTM1/P62, to verify the efficiency of autophagic flux inhibition by CQ in different strain cells and different treatments. d. CCK-8 assay was demonstrated the viabilities of T24 cells after treatment including normal, normal added CQ, starvation only and starvation added CQ (n=3, Mann-Whitney test, P* < 0.05, P** < 0.01, P*** < 0.001). e. Images of tumors in nude mice bearing T24 cells treated with normal, normal added CQ, starvation only and starvation added CQ. f. Tumor volume was measured after different treatments in nude mice every 3 days, arrow indicates the timing of intraperitoneal

administration. g and h. Cell transwell migration and invasion assay were performed in T24 and UM-UC-3 cells with different treatments (n=3, unpaired students T test, P* < 0.05, P** < 0.01, P*** < 0.001).

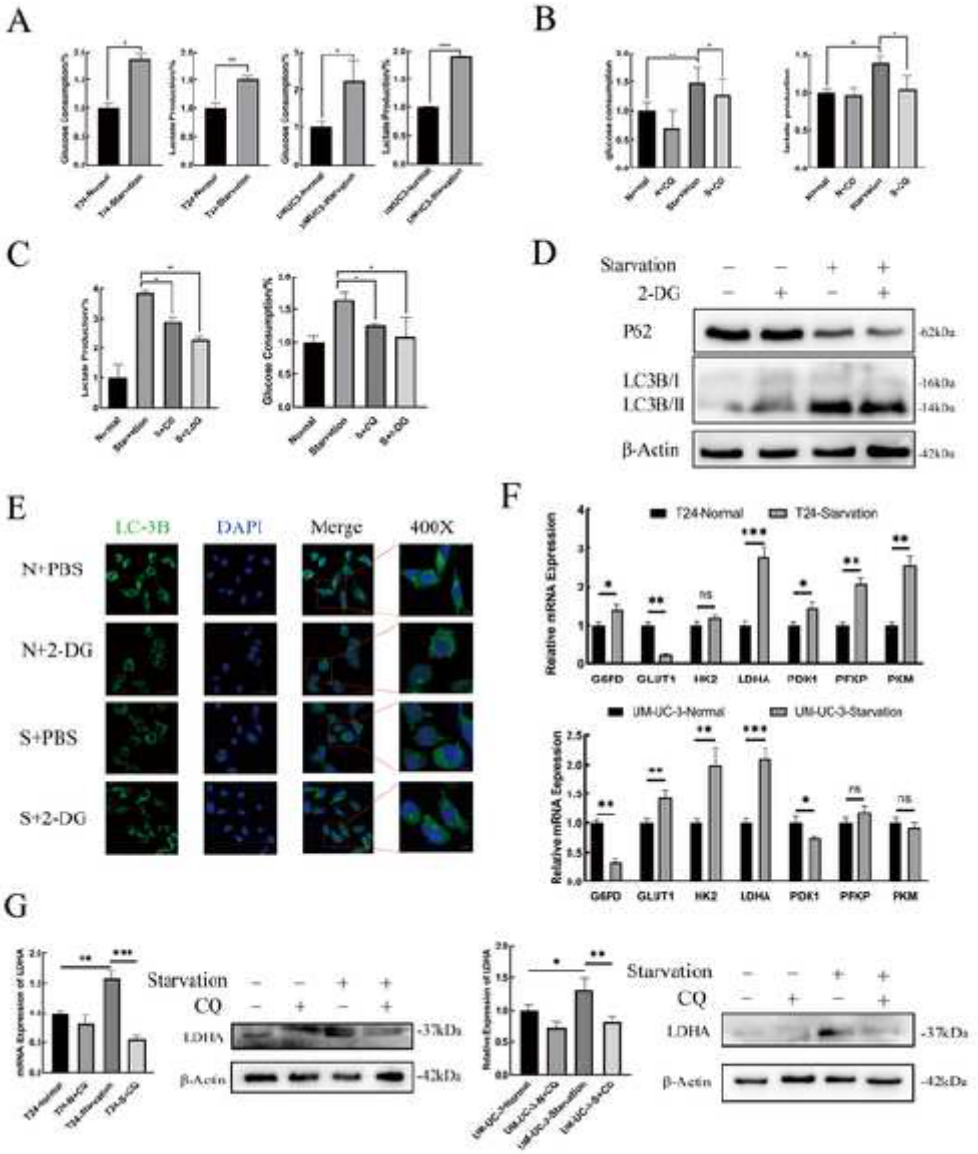

Figure 3

Starvation-induced Autophagy Regulated BC Glucose Metabolic Reprogramming by Transcriptional Overexpression of LDHA. a. Glucose consumption and lactate production ratios were measured in T24 and UM-UC-3 cells after normal or HBSS treatment, homogenized by cell counting as 104 cells (n=3, unpaired students T test, P ns > 0.05, P* < 0.05, P** < 0.01, P*** < 0.001). b and c. Glucose consumption and lactate production ratio in T24 were measured in different groups including normal, normal added CQ, starvation only, starvation added CQ or starvation added 2-DG. d. Western-blot were used to detect the changes of autophagy level, reflected by P62 and LC3B-II/I expression in T24 cells under normal, normal added 2-DG, starvation only and starvation added 2-DG treatment. e. Immunofluorescence staining of LC3B was performed in different groups T24 cells, the aggregation of LC3B represents the formation of autophagosomes. f. Real-time qPCR was performed relative expression levels of glycolysis key enzymes in T24 and UM-UC-3 cells incubated with HBSS or normal control. g. Real-time qPCR and western-blot

performed transcriptional and translational expression of LDHA in T24 and UM-UC-3 cells with different treatment, β-actin was chosen as loading control.

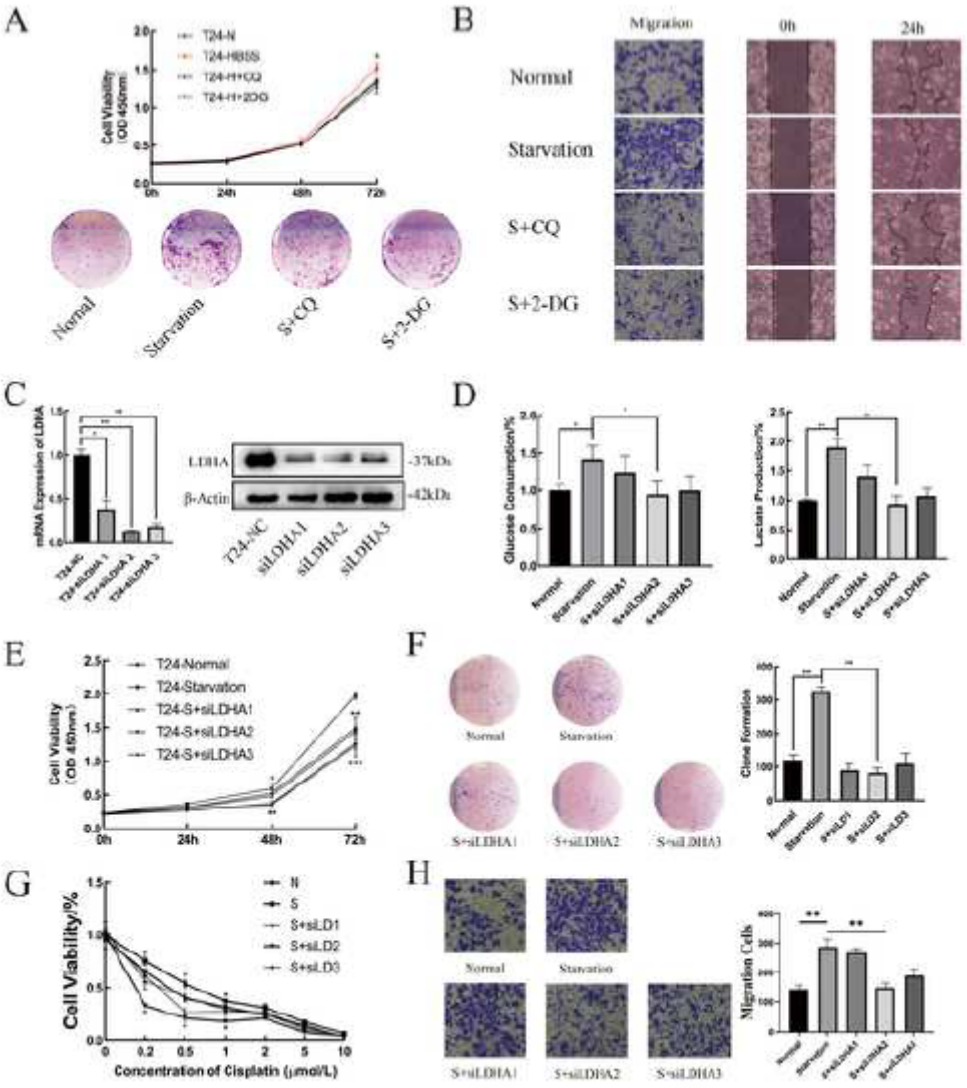

Figure 4

Starvation-induced Metabolic Reprogramming Promoted the Progression of BC by LDHA. a. Cell proliferation abilities in T24 cells with normal, starvation only, starvation added CQ and starvation added 2-DG treatment were performed by CCK-8 assay and colony forming assay (n=3, Mann-Whitney test, P* < 0.05). b. Cell migration abilities in different groups T24 cells were measured by transwell and wound healing assay. c. Real-time qPCR and western-blot performed transcription and translation expression level of LDHA in T24 cells after transfected with siRNAs, β-actin was chosen as loading control (n=3, unpaired students T test, P* < 0.05, P** < 0.01). d. Glucose consumption and lactate production ratio in T24 were measured in different groups including normal, starvation only, T24 transfected with different sequences siRNAs then cultured by HBSS, homogenized by cell counting as 104 cells. e and f. Cell proliferation abilities in T24 cells in different groups performed by CCK-8 assay and colony forming assay. g. Viabilities of T24 cells were measured after processing with graded concentrations of cisplatin

48h, cells were divided into different groups. h. Cell migration abilities in different groups T24 cells were measured by transwell assay.

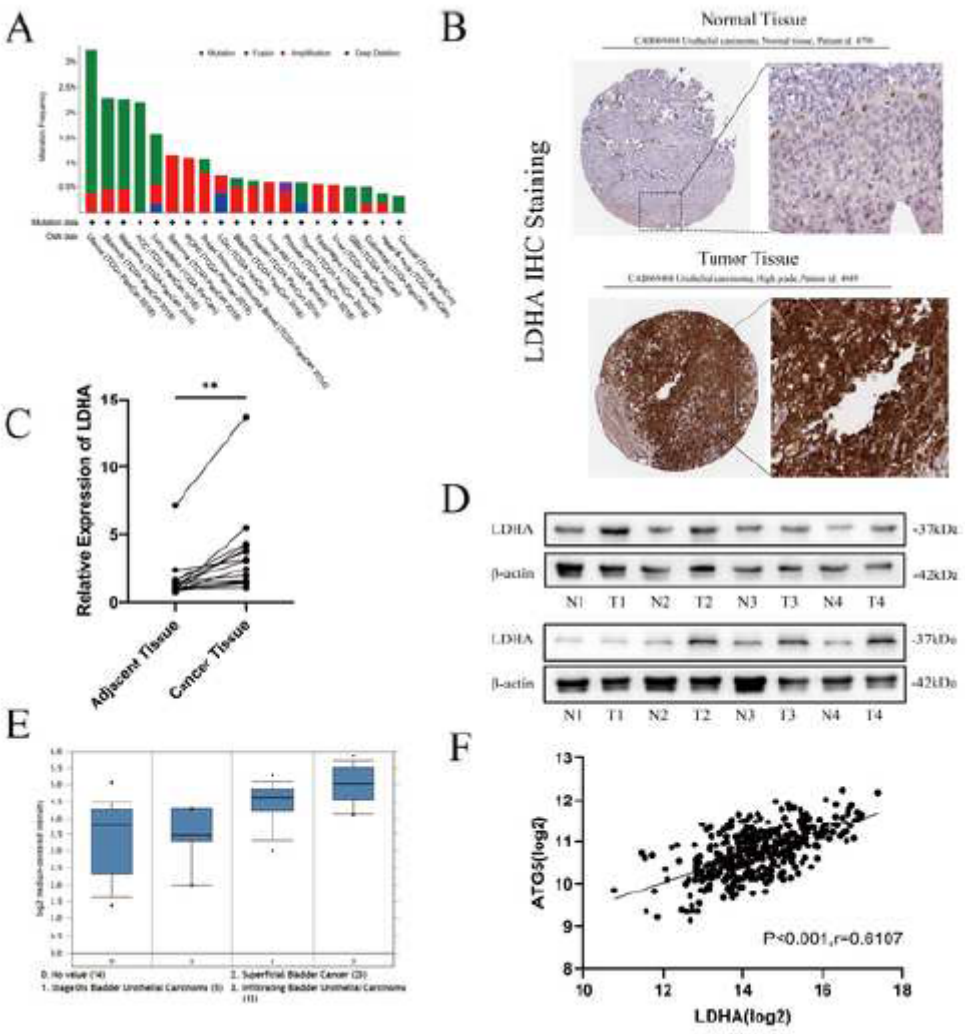

Figure 5

Overexpression of LDHA Was Closely Related to Clinical BC Patients. a. The mutation features and alteration frequency with mutation type of LDHA for the TCGA tumors were demonstrated with use of cBioPortal tool. b. Pictures of immunohistochemical staining with CAB069404 from normal bladder or BC tissue performed expression of LDHA protein in uroepithelial squamous epithelial cells. c. Real-time qPCR performed the expression of LDHA mRNA in cancer and adjacent tissues (n=15, paired students T test, P** < 0.01). d. Western-blot were performed the expression of LDHA proteins in cancer and adjacent tissues, which were randomly selected of eight paired clinical samples. e. Expression of LDHA in 60 BC patients with different depth of infiltration, sourced from Oncomine. f. The transcriptional expression relationship between LDHA and ATG5 in 378 BC tissues were analysed by Pearson correlation (r = 0.6107, P < 0.001).

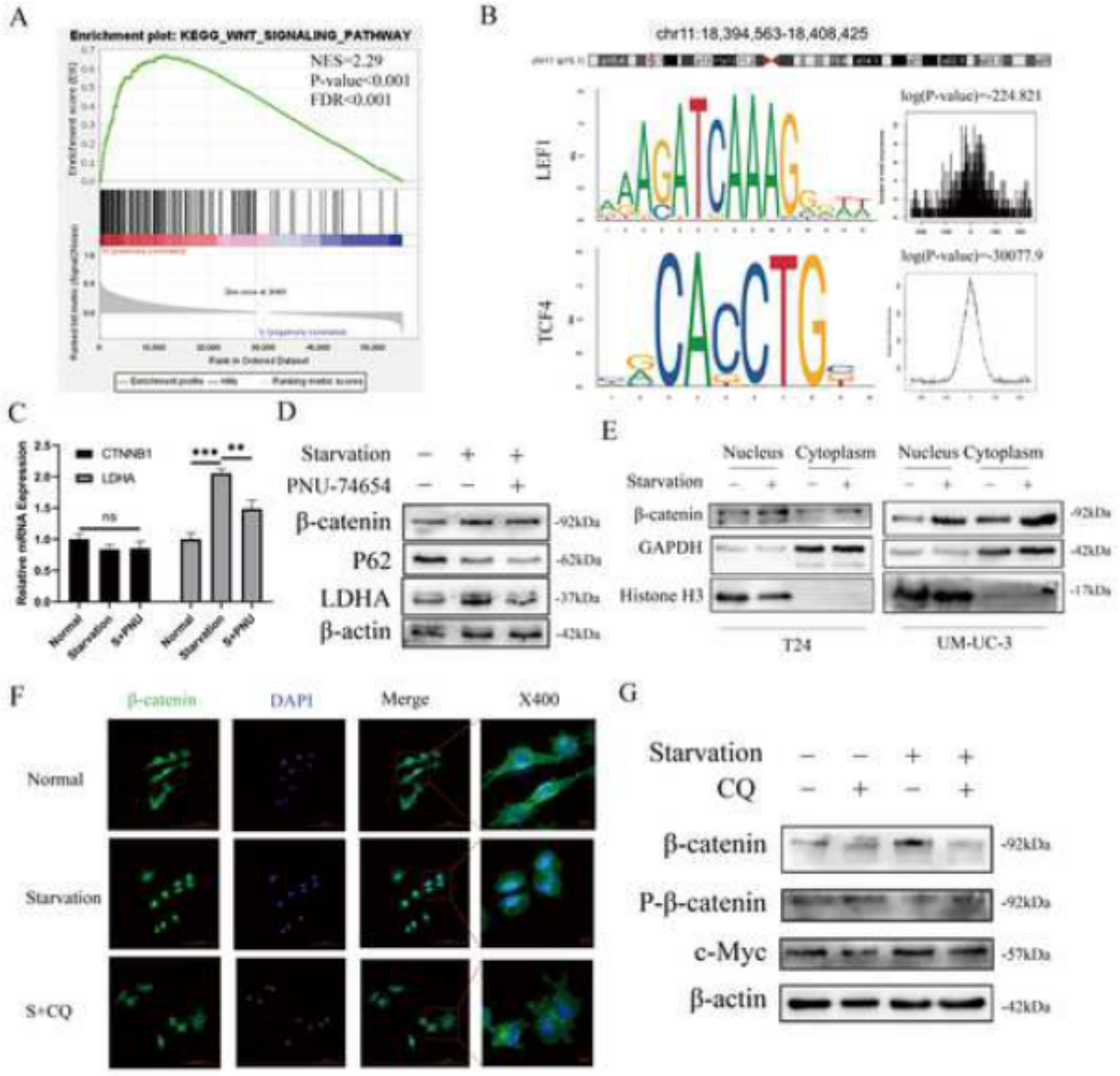

Figure 6

Starvation Regulated Expression of LDHA Through Canonical Wnt/β-catenin Pathway. a. GSEA plots were shown that the Wnt/β-catenin pathway was involved in LDHA expression in BC. b. Transcription factor binding sites of LDHA and its location on the chromosome were predicted by USUC and JASPAR. Transcription factors named LEF1 and TCF4 DNA-binding sequences were presented in human LDHA promoter region, and were demonstrated with their binding probabilities prediction respectively. c. Real-time qPCR performed the expression of LDHA and CTNNB1 at transcriptional level in T24 cells with normal incubation with DMSO, starvation added DMSO and starvation added PNU74654 (n=3, unpaired T test, P ns > 0.05, P* < 0.05, P** < 0.01). d. Western-blot were presented TCF4 up- or down-stream proteins in T24 cells with different treatment. e. Expression of β-catenin at nucleus and cytoplasm performed respectively in T24 and UM-UC-3 cells processed by starvation or not, Histone H3 were chosen to be nucleus loading control while GAPDH as cytoplasm reference. f. Immunofluorescence staining of β-catenin was performed in T24 cells treated by normal, starvation only or starvation added CQ, then

fluorescence localization was detected by confocal microscopy (scale bar, 8 μm). g. Western-blot were presented changes on different proteins expression of canonical Wnt/β-catenin pathway in T24 cells under different treatment.

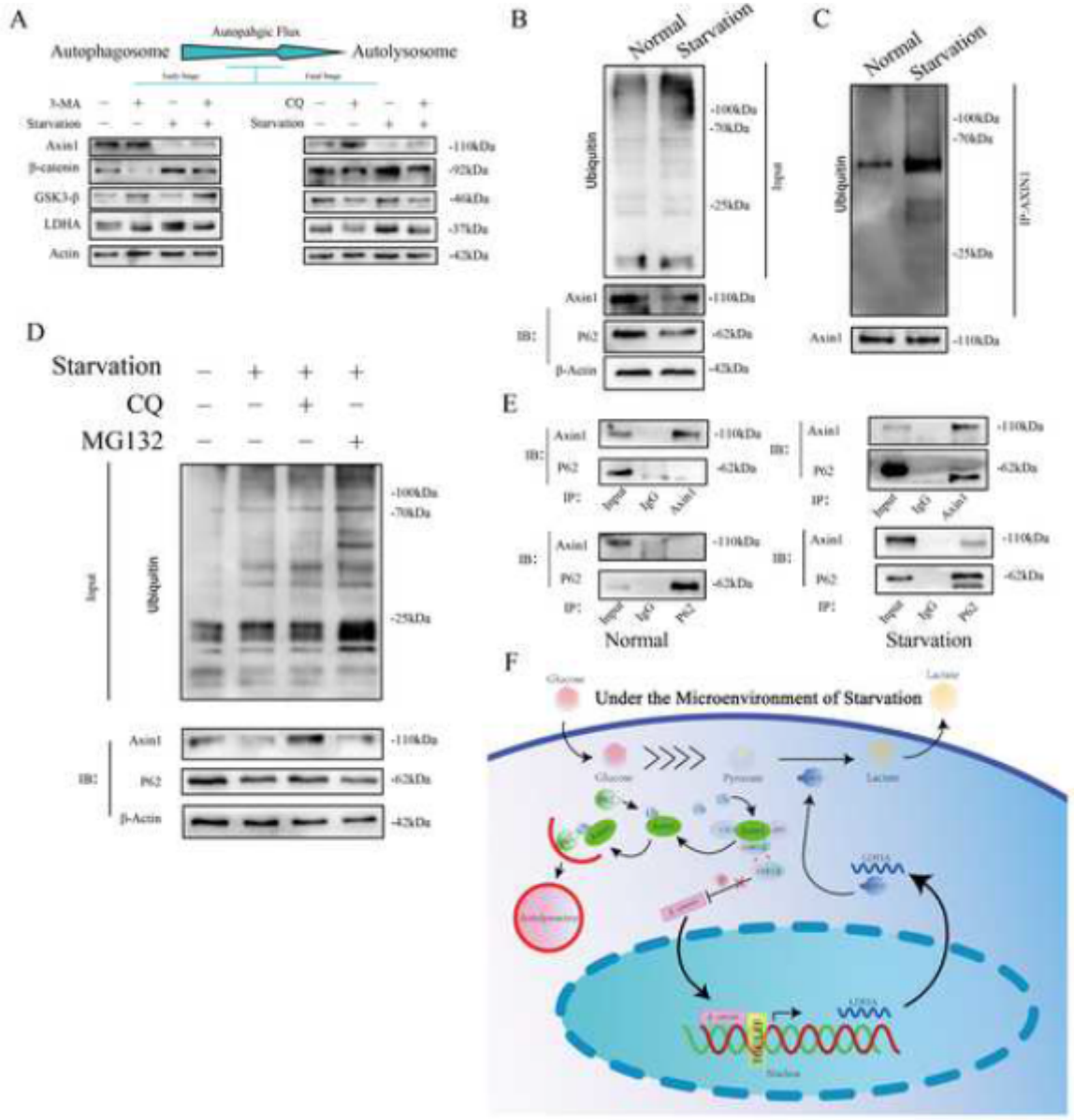

Figure 7

Starvation Regulated Wnt/β-catenin Pathway by Ubiquitination of Axin1 and Promotion of Autophagy. a. Changes of different proteins expression in T24 cells after starvation and treatment with autophagy inhibitors at different stages were detected by Western-blot. b. The amount of ubiquitination proteins in T24 cells processed by HBSS or not and expression of Axin1 and P62 performed by Western-blot. c. Anti-ubiquitin and anti-Axin1 antibody were chosen to determine ubiquitination level of Axin1. d. Western blot was performed in T24 cells incubated with HBSS or not and treated with DMSO or MG132. e. The forward and reverse immunoprecipitation were chosen to detect the interaction of Axin1 and P62 in T24 cells treated by normal or starvation. f. A schematic model of starvation induced series changes in BC.

Supplementary Files

This is a list of supplementary files associated with this preprint. Click to download.

- Sfigure.jpg
- tab01.png